

Wenyuan LI, Yu HUANG, Youmin RONG, Long CHEN, Guojun ZHANG, Zhangrui GAO

Analysis and comparison of laser cutting performance of solar float glass with different scanning modes

© Higher Education Press 2021

Abstract Cutting quality and efficiency have always been important indicators of glass laser cutting. Laser scanning modes have two kinds, namely, the spiral and concentric circle scanning modes. These modes can achieve high-performance hole cutting of thick solar float glass using a 532-nm nanosecond laser. The mechanism of the glass laser cutting under these two different scanning modes has been described. Several experiments are conducted to explore the effect of machining parameters on cutting efficiency and quality under these two scanning modes. Results indicate that compared with the spiral scanning mode, the minimum area of edge chipping ($218340 \mu\text{m}^2$) and the minimum Ra ($3.01 \mu\text{m}$) in the concentric circle scanning mode are reduced by 9.4% and 16.4% respectively. Moreover, the best cutting efficiency scanning mode is 14.2% faster than that in the spiral scanning mode. The best parameter combination for the concentric circle scanning mode is as follows: Scanning speed: 2200 mm/s, number of inner circles: 6, and circle spacing: 0.05 mm. This parameter combination reduces the chipping area and sidewall surface roughness by 8.8% and 9.6% respectively at the same cutting efficiency compared with the best spiral processing parameters. The range of glass processing that can be achieved in the concentric circle scanning mode is wider than that in the spiral counterpart. The analyses of surface topography, white spots, microstructures, and sidewall surface element composition are also performed. The study concluded

that the concentric circle scanning mode shows evident advantages in the performance of solar float glass hole cutting.

Keywords laser cutting, solar float glass, scanning mode, surface quality, cutting efficiency

1 Introduction

Solar float glass is a type of glass that reduces iron content on the basis of soda-lime glass and is widely used in architecture, medical, automotive, and flat panel display industries [1]. This type of glass is intensively used in the photovoltaic industry due to its excellent transmittance [2], and many researchers focus on how to achieve high-efficiency and high-quality processing. The scoring and breaking method is still the current mainstream glass processing method, which initially produces a scratch on the glass surface using a hard metal tool, such as a diamond cutter, and then breaks the glass along the direction of the scratch through mechanical force [3]. This method is easy to implement but will generate many microcracks and other defects on the glass cutting surface; thus, the glass edge strength is seriously weakened, and sometimes, the glass will rupture [4]. The glass surface requires additional treatment, such as polishing and grinding, but this process can only recover one-third of the strength and is time-consuming [5]. Other processing methods, such as rotary ultrasonic machining [6], abrasive water jet cutting [7], and diamond wire saw cutting [8], can successfully achieve glass cutting. However, in these methods, the quality of the glass processing surface is poor, and the efficiency is low because they are the same as the traditional processing methods of contact processing.

As a non-contact processing method, laser processing has been widely used in the processing of glass. Lumley successfully achieved the first glass processing using a CO_2 laser through a controlled fracture technique [9]. In the past few years, many studies on the laser processing of

Received March 2, 2020; accepted July 1, 2020

Wenyuan LI, Yu HUANG, Youmin RONG, Long CHEN,
Guojun ZHANG (✉)

State Key Laboratory of Digital Manufacturing Equipment and Technology, Huazhong University of Science and Technology, Wuhan 430074, China; School of Mechanical Science and Engineering, Huazhong University of Science and Technology, Wuhan 430074, China
E-mail: zhanggj.hust@gmail.com

Zhangrui GAO
HG Farley Laserlab Cutting Welding System Engineering Co., Ltd.,
Wuhan 430223, China

glass have been conducted, and many cutting methods are proposed [10]. The laser scoring and breaking method is similar to the conventional scoring and breaking method, except that a certain depth of grooves is created by the laser beam acting on the glass, and other mechanical forces are used to break the glass [11]. In this method, the problem of poor glass edges still exists, and an additional processing procedure is required. Some researchers used the laser melting and evaporation method to cut glass. However, this method not only results in the poor surface finish but also requires additional grinding and polishing process because the cutting procedure is above the glass transition temperature [10,12]. Laser-induced thermal-crack propagation is a type of cutting method that can achieve high cutting quality and efficiency without any subsequent cleaning and grinding. In this method, the material absorbs the laser photon energy to raise the temperature and generate compressive stress. Then, the processing area cools to generate residual stress as the laser beam moves. If these stresses exceed the failure stress, then a crack occurs and propagates along the direction of the laser beam movement [10]. At present, this method has been widely used in cutting glass [1,13] and other transparent materials [14]. However, the leading and trailing edges of the glass sheet sometimes have a cutting deviation. Hence, researchers proposed the multiple laser system [15] and dual-laser beam method [16,17] to revise the cleaving path and obtain a stable fracture on the surrounding region of the laser moving path with laser-induced thermal-crack propagation. Moreover, the glass sheets with straight and curved fractures were simulated and realized using the circular microwave spot with the thermal-controlled fracture method because the microwave heat source can be used to heat the inner part of glass sheets at low temperatures [18]. The ultrashort pulse laser processing methods, such as femtosecond laser cutting [19,20] and femtosecond filamentation [21] processing, become highly extensive in glass processing with a high cutting quality due to minimal thermal effects. A feasible chemically strengthened glass separation technique by integrating picosecond laser ablation with quenching-induced thermo-shock has been developed and demonstrated. Through this method, various enclosed shapes with the surface roughness are successfully separated, and the chipping level can satisfy the requirement [22]. However, this method is limited by the thickness of glass and is suitable for micromachining due to its high cutting quality [23,24]. A flexible laser multi-focus separation technology was proposed to address the problem of laser processing of thick glass. A high-quality edge cutting of 20-mm soda-lime glass was achieved using this method because the temperature and thermal stress are evenly distributed by producing multi-focus along with the thickness of the material [25]. The laminated glass with a very smooth sidewall was also successfully separated using three laser foci acting on each layer, without any separation defects,

such as chipping, microcracks, or subsurface damage [26].

The photovoltaic industry needs to punch holes in glass for threading. The main method currently adopted is mechanical drilling, but the cutting efficiency is not high enough due to the high hardness and brittleness of the glass, and this method can cause serious chipping at the glass edge. Chipping is always an important indicator of the quality of glass processing [27]. Moreover, facing the demand for various shaped holes in the industry and the trend of thin and light glass, traditional processing methods are difficult to handle. At present, the main objective of glass laser processing is glass separation, and laser cutting of thick glass is less studied. This study mainly discusses the thick solar float glass through the hole laser cutting method, which realizes high-quality and high-efficiency glass cutting by using different laser scanning modes. Analysis and comparison of cutting quality and efficiency under different scanning modes were implemented. Based on this, the laser cutting performance was improved.

2 Principle

Figure 1 shows the basic principle of solar float glass laser cutting. The bottom-up cutting method was adopted to maximize the high transmittance and the characteristics of volumetric absorption of solar float glass for the laser beam with a wavelength of 532 nm [1]. The focus laser spot was placed under the lower surface of the glass, and the circle of specified size on the X - Y plane was completely scanned. Then, the laser focus raised a certain distance in the Z -axis direction, and the same path on the next plane was scanned until the entire glass thickness was finished. However, the kerf produced by laser scanning at only one circle per plane is very small, which is not enough to eliminate the glass cutting powder in time, eventually resulting in the cutting failure. Two different filling modes exist, namely, spiral and concentric circle scanning modes. Both are useful to achieve glass cutting. Figure 1 shows that the laser beam emitted by the laser source enters the galvanometer after passing through two reflecting mirrors and finally is focused under the low surface of the glass by the lens. The spiral scanning path is a series of large semicircles with a certain radius and area overlapping degree and small semicircles connecting adjacent large semicircles to form a continuous spiral. The parameter relationship is shown as follows:

$$w = 2R - \frac{D}{2}, \quad (1)$$

$$r = \frac{2R^2 \arccos \frac{D}{2R} - D \sqrt{R^2 - \frac{D^2}{4}}}{\pi R^2}, \quad (2)$$

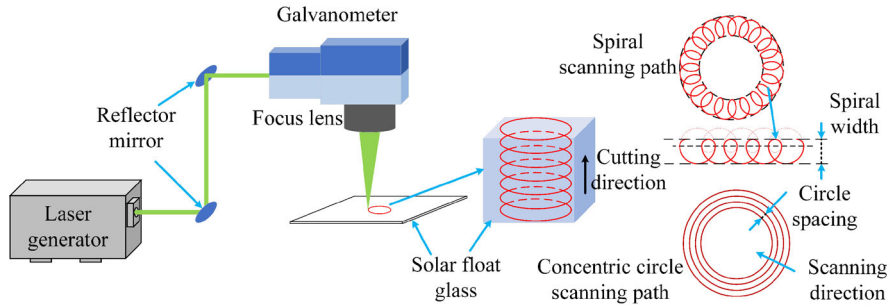


Fig. 1 Schematic of solar float glass laser cutting under different scanning modes.

where w is the spiral width, r is the spiral overlap ratio, R is the radius of a large semicircle, and D is the center distance between two adjacent large semicircles.

The concentric circle scanning mode is to insert a certain number of concentric patterns with a certain spacing inside the cutting pattern to ensure a certain width of the cutting kerf.

Both laser scanning modes are based on the above-mentioned characteristics of high transmittance of glass and volumetric absorption of a 532-nm wavelength laser by the glass, and the glass laser hole cutting is realized with a controlled fracture technique [1]. Figure 2 shows that when the laser spot acts on glass, a high temperature (not exceeding the glass transition temperature) is generated, and then, compressive stresses are produced in the heating area. As the laser beam moves, these compressive stresses are relaxed due to convection cooling of air in this region and induce residual tensile stresses. When the residual tensile stresses are greater than the failure strength of glass, microcracks will occur. Furthermore, the crack propagates along with the scanning path of the laser beam, which breaks the glass into powder and eliminates it, thereby forming a kerf.

The mechanism of each layer of laser focus acting on the glass to produce a kerf with a certain width is different. For the spiral scanning mode, when the laser scans along this path, the glass generates microcracks along the scanning trajectory and breaks the glass into powder within the spiral width. However, the formation process of the kerf is to produce a kerf with a certain width from the starting point of cutting and gradually complete the entire kerf along the circumference of the cut hole. The spiral track overlaps to achieve full erosion of the material in the kerf. For the concentric circle scanning mode, the kerf is formed by inserting several circles of the same pattern with a certain circle spacing into the hole. The kerf forming process is different from the spiral scanning mode. First, the laser scans directly once to generate a kerf with a certain width across the circumference. As the laser sequentially scans the same trajectory in the pattern, the entire kerf width is continuously expanded until a smooth discharge of glass cutting powder is ensured. The circle

spacing with a certain value determines the degree of overlap of the kerfs produced by the laser in the adjacent scanning path.

Glass chipping greatly affects the processing quality and thus is often used as an indicator to measure laser-processed glass edge quality. However, Fig. 2 shows that when the laser is applied to the glass surface, the microcracks produced by thermal effect propagate toward both sides of the kerf. Moreover, the maximum principal stress generated exceeds the strength limit of the glass, which will cause chipping at the glass surface edge.

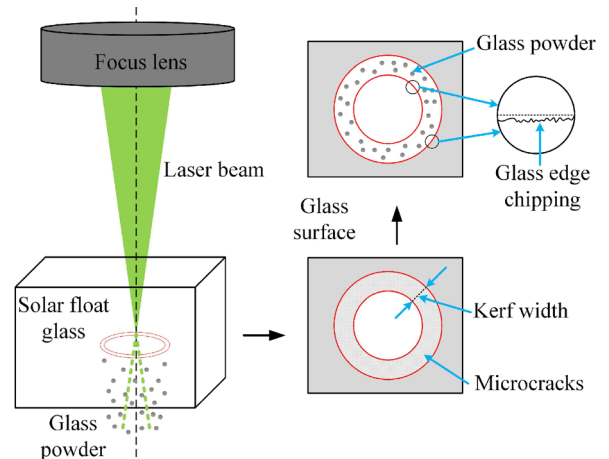


Fig. 2 Schematic of glass chipping formation by laser cutting.

3 Experimental procedure

3.1 Materials

Solar float glass (provided by CSG Holding Co., Ltd., China) was chosen as the material of this experiment because of its extensive application in the photovoltaic industry and its excellent transmittance. The composition of solar float glass is 72% SiO_2 , 13.1% Na_2O , 7.95% CaO , 4.45% MgO , 1.15% Al_2O_3 , 0.5% K_2O , 0.22% SO_2 , and 0.01% Fe_2O_3 . Table 1 shows the physical and mechanical properties of solar float glass.

Table 1 Physical and mechanical properties of solar float glass

Properties of solar float glass	Value
Density	2480 kg/m ³
Expansion coefficient	9.1 × 10 ⁻⁶ /K
Specific heat capacity	836 J/(kg·K)
Thermal conductivity	0.8 W/(m·K)
Young's modulus	74 GPa
Poisson's ratio	0.23
Softening temperature	993–1003 K
Average bending fracture strength	49 MPa

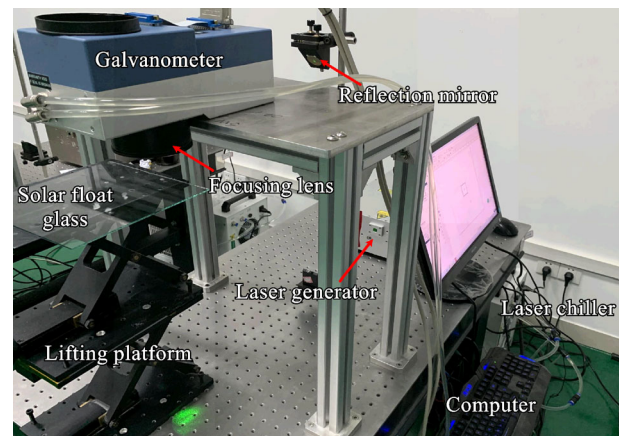
3.2 Experimental setup

Figure 3 depicts the experimental apparatus for solar float glass laser cutting. A Nd:YVO₄ nanosecond solid laser (LOGAN type LNS-532-40 PRO) with a wavelength of 532 nm (laser beam was near Gaussian and $M^2 \leq 1.2$) was used in this experiment. A high-precision 3D galvanometer (Anshan Precision 3D Post-Scanning System) with 1.67 times beam expansion was used to achieve different scanning paths. An f-theta focusing lens (CARMAN HAAS type SL-532-50-65) with a scanning range of 50 mm × 50 mm and a focal length of 65 mm was used in focusing the laser beam. The glass sheet was placed on a Z-axis precision lifting platform after its surface was cleaned, and the glass area to be processed was suspended above the laser focus. In addition, a vacuum cleaner was fixed under the glass sheet to collect the glass cut powder.

3.3 Experimental design

The Taguchi method L₁₆ was carried out with two laser beam scanning modes under the same laser power. Experimental parameters include scanning speed, spiral width, and spiral overlap ratio for spiral scanning mode and scanning speed, number of inner circles, and circle spacing for the concentric circle scanning mode, respectively. The appropriate pulse frequency value (43 kHz, single pulse energy 590 μJ) is selected as the laser energy basis of the two scanning modes. Scanning speed is an important processing parameter which determines the overlapping rate of laser pulses. The other parameters determine the scanning path of the laser in the two scanning modes. The two scanning modes are layer-by-layer scanning in the vertical direction of the glass. Thus, the laser focus rise distance per layer is set to a certain appropriate value to reduce its influence on processing quality. Each parameter has four levels that were selected uniformly within the range that glass processing can be successfully achieved (except the number of inner circles, its continued increase can still achieve glass cutting but will not significantly affect the cutting quality, while

seriously reducing the cutting efficiency). Table 2 shows the experimental parameters and their levels, and Table 3 shows the other details of laser cutting solar float glass conditions. This experiment selected the square hole as the shape of cutting specimen to facilitate the measurement of the glass edge chipping and the surface quality of the hole sidewall. Each group of experiments was conducted five times to reduce random error.

**Fig. 3** Experimental setup for laser cutting of solar float glass.**Table 2** Process parameters and their levels

Scanning mode	Parameter	Value
Spiral scanning mode	Scanning speed, v	200, 250, 300, and 350 mm/s
	Spiral width, w	0.45, 0.5, 0.55, and 0.6 mm
	Spiral overlap ratio, r	60%, 65%, 70%, and 75%
Concentric circle scanning mode	Scanning speed, v	1600, 1900, 2200, and 2500 mm/s
	Number of inner circles, n	5, 6, 7, and 8
	Circle spacing, d	0.04, 0.05, 0.06, and 0.07 mm

Table 3 Processing condition of solar float glass by laser cutting

Property	Value
Shape and size of specimens	Square, 8 mm × 8 mm × 2.2 mm
Laser pulse frequency	43 kHz
Laser power under focus lens	25.4 W
Focus spot size	15 μm
Focus rise distance per layer	0.02 mm
Laser chiller constant temperature	23 °C
Ambient temperature	25 °C
Chiller cooling water	Deionized water

3.4 Measurement

The square glass cut was used as research specimens to analyze of the cutting quality. The glass edge chipping situation was evaluated by the area of the chipping. The chipping and the surface roughness of the sidewall were investigated using a laser confocal microscope (VK-X200K, KEYENCE Corporation, Japan). One side of the glass edge was chosen randomly, and each specimen was placed in the middle of the microscope field horizontally to measure the area of the chipping and the maximum chipping width over a length of 2909.1 μm . The surface roughness of the laser-processed sidewall was also measured using the laser confocal microscope. The microstructures of the laser-processed sidewall were observed using a field emission scanning electron microscope (SEM: Sirion 200, FEI Company, USA), and the specimens were sprayed with gold using an ion-sputtering instrument (SBC-12, KYKY Technology Co., Ltd., China) for 90 s before observation because the glass is not

conductive. In addition, the elemental content of the laser-machined surface was also detected through energy dispersive spectrometer (EDS) using the same SEM. Given that the distance of focus rise per layer was kept constant, the number of layers that need to be scanned in the thickness direction of the glass is a fixed value. During the laser cutting process, several layers are added to the upper and lower surfaces of the glass to ensure sufficient cutting. The cutting time was used to measure the cutting efficiency and can be obtained by controlling the laser and galvanometer software.

4 Results and discussion

After a series of experiments with different cutting parameters, as shown in Fig. 4, two different laser scanning modes have achieved glass hole laser cutting with a high edge and sidewall quality. Tables 4 and 5 show the experimental results.

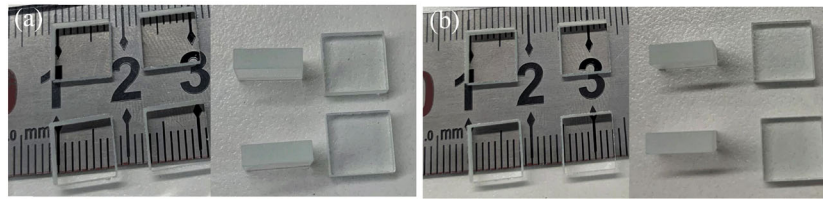


Fig. 4 Machined specimens with different laser scanning modes: (a) The spiral scanning mode with parameter combination No. 12 in Table 4; (b) the concentric circle scanning mode with parameter combination No. 12 in Table 5.

Table 4 Experimental results in the spiral scanning mode

No.	$v/(\text{mm} \cdot \text{s}^{-1})$	w/mm	$r/\%$	Chipping area/ μm^2	$Ra/\mu\text{m}$	Cutting time/s
1	200	0.45	60	363036	8.76	20.31
2	200	0.50	65	364899	6.22	20.31
3	200	0.55	70	474649	6.25	20.31
4	200	0.60	75	380659	4.27	20.31
5	250	0.45	65	363388	7.32	16.32
6	250	0.50	60	442924	7.25	16.32
7	250	0.55	75	447636	3.62	16.32
8	250	0.60	70	306502	6.15	16.32
9	300	0.45	70	399383	4.96	13.65
10	300	0.50	75	481037	4.51	13.65
11	300	0.55	60	295180	4.57	13.65
12	300	0.60	65	241009	3.66	13.65
13	350	0.45	75	457950	3.98	11.75
14	350	0.50	70	384307	3.60	11.75
15	350	0.55	65	479588	7.33	11.75
16	350	0.60	60	471696	9.67	11.75

Note: Ra , surface roughness.

Table 5 Experimental results in the concentric circle scanning mode

No.	$v/(mm \cdot s^{-1})$	n	d/mm	Chipping area/ μm^2	$Ra/\mu m$	Cutting time/s
1	1600	5	0.04	424832	3.48	15.51
2	1600	6	0.05	416584	3.50	17.85
3	1600	7	0.06	323467	3.98	20.08
4	1600	8	0.07	405490	4.19	22.19
5	1900	5	0.05	341807	3.20	13.12
6	1900	6	0.04	434733	3.56	15.30
7	1900	7	0.07	386704	3.19	16.96
8	1900	8	0.06	304975	3.01	19.07
9	2200	5	0.06	401814	4.21	11.38
10	2200	6	0.07	244576	4.63	13.08
11	2200	7	0.04	341502	3.71	15.17
12	2200	8	0.05	218340	3.24	16.79
13	2500	5	0.07	413602	4.60	10.08
14	2500	6	0.06	380233	4.48	11.72
15	2500	7	0.05	320253	4.82	13.37
16	2500	8	0.04	360403	3.62	15.07

Note: Ra , surface roughness.

4.1 Comparison of chipping area, surface roughness, and cutting time results

Tables 4 and 5 show that under the same laser power, although other parameters are different, the overall glass chipping area in the concentric circle scanning mode is smaller than that in the spiral scanning mode. Compared with the spiral scanning mode, the minimum and the maximum area of edge chipping are reduced by 9.4% and 9.6% in the concentric circle scanning mode, respectively. The surface roughness (Ra) of the laser-processed sidewall in two scanning modes is quite different, and the overall Ra value is smaller in the concentric circle scanning mode than in the spiral scanning mode. Furthermore, the minimum Ra of the concentric circle scanning mode is 16.4% smaller than that of the spiral scanning mode. For cutting efficiency, the overall cutting time of the two scanning modes is comparable, but the best cutting efficiency is 14.2% faster than the spiral scanning mode in the concentric circle scanning mode.

4.2 Effect of process parameters on the chipping area and Ra

Grey correlation analysis is used to analyze the relationship between parameters, glass edge chipping area, and Ra of laser-processed sidewall due to the complex interaction between the laser and glass in different laser scanning modes. The grey correlation degree values of three parameters, the glass edge chipping area, and Ra are calculated by using MATLAB software, as shown in Table 6.

The order of the gray correlation degree of the three parameters on the chipping area and Ra is $\gamma_w > \gamma_r > \gamma_v$ and $\gamma_r > \gamma_w > \gamma_v$, respectively, in the spiral scanning mode, and that of concentric circle scanning mode is $\gamma_d > \gamma_v > \gamma_n$ for both indicators. Therefore, the main factors that affect the cutting quality of the spiral scanning mode are the parameters of w and r , and the influence of d is particularly evident for the concentric circle scanning mode.

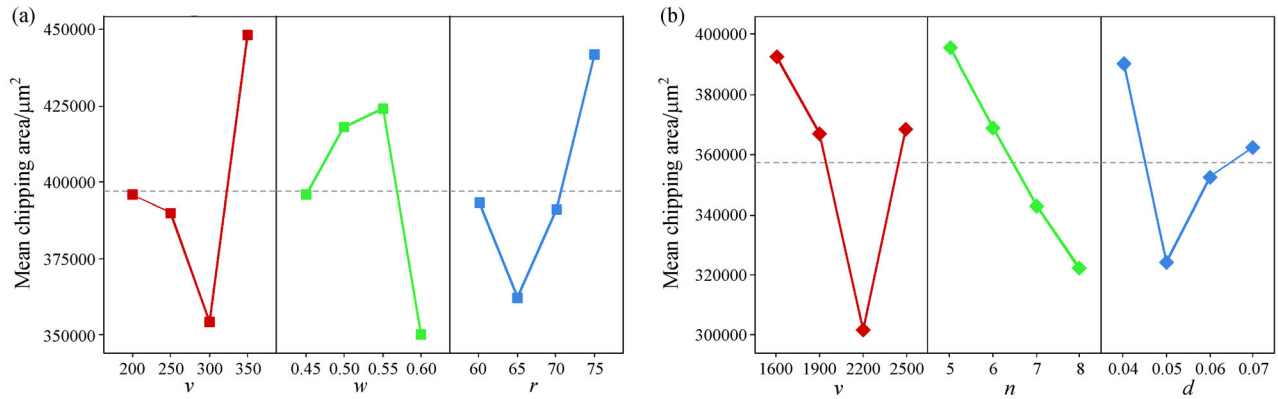
4.2.1 Influence trend of parameters on chipping

Figure 5 shows that in two different laser scanning modes, the edge chipping area decreases with the increase of v and begins to increase when a threshold value is reached. When v is lower than the threshold, the pulse overlap rate will be too high. Moreover, significant heat accumulation produces a high temperature so that enough tensile stress is generated to make additional non-uniform fracture at the edge of the glass, thereby increasing the glass chipping area. On the contrary, when the v value is greater than the threshold, the laser energy action time will be shortened. In this case, the tensile stress generated by the low temperature is insufficient to form a stable kerf along the scanning path and will cause uneven damage at the edges of the glass, so the glass chipping area is also increased.

For the spiral scanning mode, the chipping area increases as w increases and begins to decrease as soon as a certain point is reached. This result may be because when w is lower than the turning point, the spiral path is tight, so that the energy of the laser on the edge of the glass is relatively uniform, thus improving the chipping situation. When w is greater than the turning point,

Table 6 Gray correlation degree of three parameters with chipping area and Ra

Scanning mode	γ_v	γ_w	γ_r	γ_n	γ_d
Spiral scanning mode					
Chipping area	0.605	0.690	0.681		
Ra	0.577	0.595	0.639		
Concentric circle scanning mode					
Chipping area	0.633			0.596	0.654
Ra	0.613			0.592	0.651

**Fig. 5** Effect of parameters on glass chipping in different scanning modes: (a) Spiral scanning mode; (b) concentric circle scanning mode.

although the spiral is not tight enough, the small semicircles in the spiral becomes larger. Furthermore, the laser energy area is uniform, and the kerf is wide making the removal of the cutting powder in time easy, thereby reducing the influence on the glass edge chipping. The r value directly affects the density of the spiral scan path, extremely large or small will make the laser energy in the spiral path distribution inappropriate and increase the chipping area.

For the concentric circle scanning mode, the glass chipping area decreases as n increases and decreases as the d increase, and then, the area starts to increase when a certain turning point is reached. If the n is large, then the kerf is also large, and removing the glass cutting powder is easy. The d value also affects the density of the laser energy path distribution. A value larger or smaller than the critical value will increase the glass chipping area.

Figure 6 shows that the cutting parameters of two scanning modes interacted with each other for the chipping area, and some trends can be summarized through the analysis line. For the spiral scanning mode, $v*w$: The entire fluctuation of v (approximately 300 mm/s) on the chipping area was sharper than that of other levels; $v*r$: The r value at 65% had a substantial influence on the chipping area, and that with 75% had a weak effect; $w*r$: The strong fluctuation occurred on the w at 0.6 mm, and that of the other four levels changed relatively smoothly. For

concentric circle scanning mode, $v*n$: The sharp fluctuation occurred at 2200 mm/s of v , whereas the n value at level 7 had limited influence; $v*d$: The d value at 0.06 mm had gentle fluctuation compared with other levels; $n*d$: The strong fluctuation occurred in levels 6 and 8 of n , whereas the n value at levels 5 and 7 has a limited effect.

4.2.2 Influence trend of parameters on Ra

Figure 7 shows that the effect of v on the surface roughness of the laser-processed sidewall is the same as that on the chipping area. Only a suitable v value is beneficial to the distribution of the laser energy, thus improving the quality of the cutting surface. A small w is not conducive to the timely removal of glass cut powder and affects the quality of the cutting surface. In addition, a large width will make the spiral trajectory extremely sparse and cause uneven cutting energy in the kerf, thereby leading to big surface roughness. The surface roughness of a laser-processed sidewall decreases with the increase of r because when the overlap ratio of the spirals is low, the special trajectory creates evident wavy stripes on the sidewall surface of the glass, which increases the surface roughness. As the overlap rate increases, this phenomenon will gradually disappear, and the surface roughness will be reduced.

In the concentric circle scanning mode, n has less effect on the quality of the cutting surface. Several inner circles

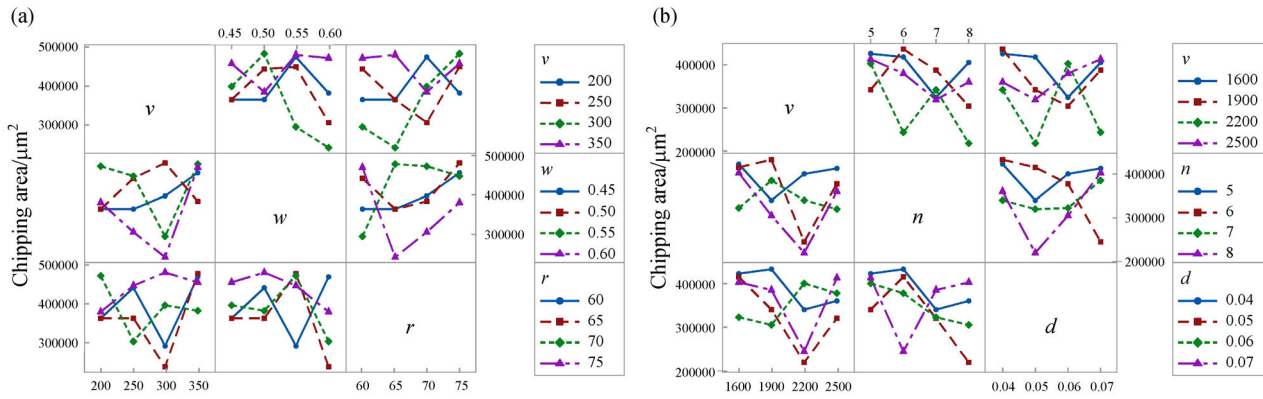


Fig. 6 Interactions between each cutting parameter for the chipping area in different scanning modes: (a) Spiral scanning mode; (b) concentric circle scanning mode.

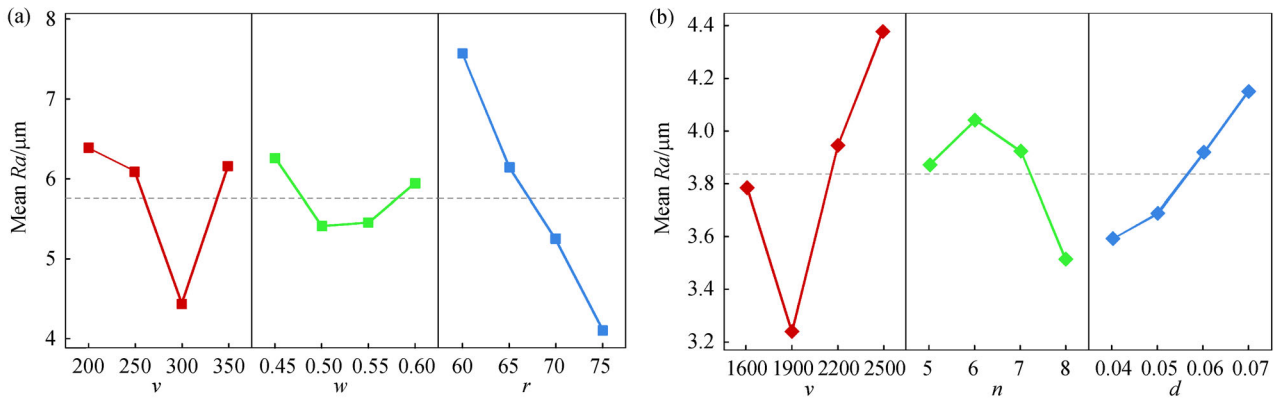


Fig. 7 Effect of parameters on Ra in different scanning modes: (a) Spiral scanning mode; (b) concentric circle scanning mode.

mean a wide width of the kerf, which is conducive to the discharge of residues and improves the roughness of the cutting surface but will greatly reduce the cutting efficiency. If the d is large, then the roughness may be great because the d value determines the degree of sparseness for this scanning method. As d increases, the zone between adjacent two circles will be cut insufficient, resulting in some white spots on the cutting surface and increasing roughness.

Figure 8 depicts the interaction between the parameters of two scanning modes for sidewall Ra . For the spiral scanning mode, v^*w : The v value at 350 mm/s had a great influence on Ra , and that with 300 mm/s possessed a weak effect; v^*r : The Ra value decreased gradually with the increase of r , whereas an unexpected fluctuation was presented in the v fourth level of 350 mm/s; w^*r : The r value at 75% had a weak effect on Ra . The strong fluctuation occurred on the w level of 0.6 mm. For the concentric circle scanning mode, v^*n : The gentle fluctuation occurred in level 8 of n and at 1900 mm/s of v ; v^*d : Compared with the other three levels, the d value at 0.04 mm had an extremely weak effect on Ra ; n^*d :

Similarly, the gentle fluctuation occurred on the d level of 0.04 mm. The n value at level 8 had a limited influence on Ra .

4.3 Influence trend of process parameters on cutting efficiency

Figure 9 shows the effect of different parameters on cutting efficiency under two laser scanning modes. For the spiral scanning mode, the parameters of w and r have no effect on the cutting efficiency may be because the overall scanning path length slightly changes when w and r change for the relatively fast v . Therefore, the cutting efficiency depends entirely on v (focus rise distance per layer remains constant). However, the change of the cutting time with v is not completely linear, which may be caused by the idle time of each layer of cutting and the delay time of the laser on and off. The effect of v on cutting efficiency in the concentric circle scanning mode is the same as that in the spiral scanning mode. The effect of n on cutting efficiency is very significant. Figure 9(b) depicts that the scanning time is proportional to n . Several inner circles mean a long

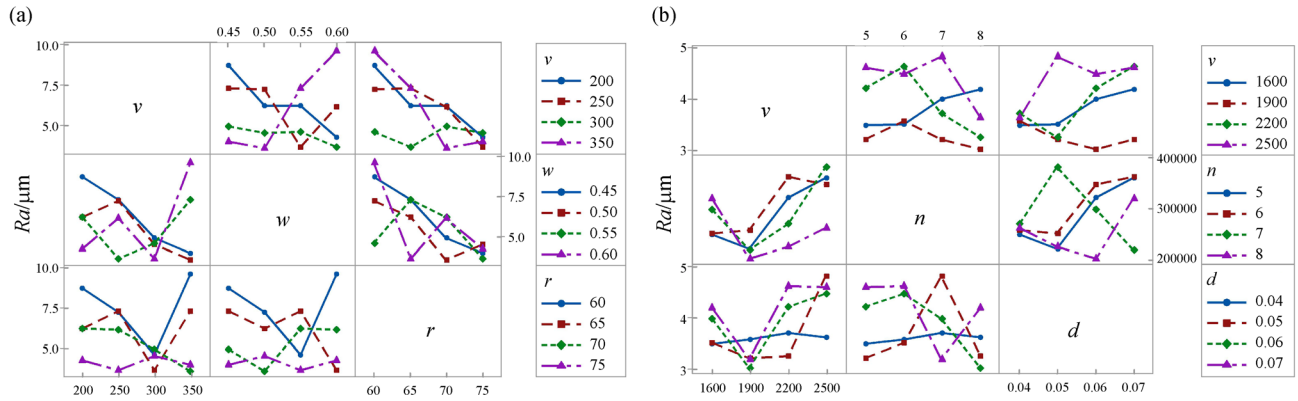


Fig. 8 Interactions between each cutting parameter for Ra in different scanning modes: (a) Spiral scanning mode; (b) concentric circle scanning mode.

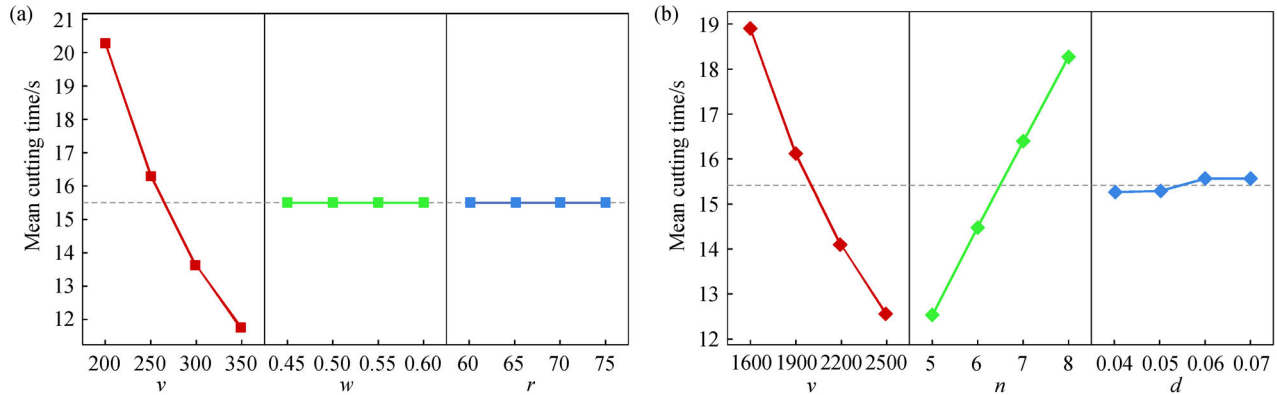


Fig. 9 Effect of parameters on cutting efficiency in different scanning modes: (a) Spiral scanning mode; (b) concentric circle scanning mode.

laser scanning path. In addition, the reduced circumference of the inner circles can be ignored at a relatively fast v due to the relatively small d . The effect of d is negligible, but the cutting time tends to increase as d increases because the low galvanometer idle speed can cause a small change in cutting time for many circle spacings.

According to the above grey correlation, the main effect and interaction effect analysis, the best combination of process parameters in our experiments for improving cutting performance is v (300 mm/s), w (0.6 mm), and r (65%) in the spiral scanning mode. The chipping area of this parameter combination in the experiment is the smallest (241009 μm^2), and simultaneously, the surface roughness of the laser-processed sidewall is also very small (3.66 μm), and the cutting efficiency is also high (13.65 s). For the concentric circle scanning mode, the edge chipping area is given priority because the overall fluctuation of the roughness of the processed surface is small. The best parameter combination is v (2200 mm/s), n (8), and d (0.05) with the smallest chipping area (218340 μm^2) and a

small Ra (3.24 μm). However, the efficiency of this group is quietly low (16.79 s). Considering the cutting efficiency, combined with the analysis results, the parameter combination of v (2200 mm/s), n (6), and d (0.05) is selected as a great group of parameters. However, this group of parameters did not appear in the experiment. After experimental verification, the average chipping area is 219865 μm^2 , the surface roughness of the cut hole sidewall is 3.31 μm , and the cutting efficiency is also high (approximately 13.08 s). This result means that under the same cutting efficiency, the concentric circle scanning mode reduces the chipping area and sidewall surface roughness by 8.8% and 9.6%, respectively, compared with the spiral scanning mode.

4.4 Analysis of surface topography

4.4.1 Chipping area

Figure 10 shows the minimum chipping area in two

scanning modes. In the concentric circle scanning mode, the chipping is more uniform, and the maximum chipping width ($129.26\ \mu\text{m}$) is smaller, compared with those in the spiral scanning mode ($181.82\ \mu\text{m}$). This finding means that at the same laser power, the concentric circle scanning mode can effectively reduce the chipping of the glass edge compared with the spiral scanning method.

Figure 11 depicts the contour curve of the glass height on a horizontal line in the glass chipping area. The height fluctuation of the spiral scanning mode in the chipping area is greater than that of the concentric circle scanning mode, where the maximum difference between the height in the spiral and concentric circle scanning modes is 166.56 and $122.35\ \mu\text{m}$, respectively. This result shows that the degree of damage to the glass in the glass chipping area of the concentric scanning method is less than that in the spiral scanning mode.

Figure 12 illustrates the maximum chipping area caused by two different scanning modes. The glass chipping situation is serious, the width of the chipping also becomes uneven, and the maximum chipping is $288.35\ \mu\text{m}$. The chipping situation is severe under the spiral scanning mode, has a large chipping width (maximum $438.92\ \mu\text{m}$),

and has many white spots on the cutting sidewall. During the cutting process, when uneven energy distribution or cutting powders are not discharged in time, the stress generated by the laser on the glass is insufficient, thus cannot crack the glass into a powder and discharge, or partially melting the glass thereby leading to the formation of white spots.

4.4.2 Surface topography of laser-processed sidewall

Figure 13 depicts the three-dimensional topography of the laser-processed sidewall surface with minimum surface roughness values in two scanning modes. Both surfaces are smooth, but the surface quality is better under the concentric circle scanning mode than the spiral counterpart. Figure 14 shows that from the three-dimensional topography of the laser-processed sidewall with large R_a , the surface quality under concentric circle scanning mode is better than that of the spiral scanning mode, and the surface under the spiral scanning mode is not smooth enough and has large white spots. The surface quality of the laser-processed sidewall in the concentric circle scanning mode is better than that in the spiral scanning

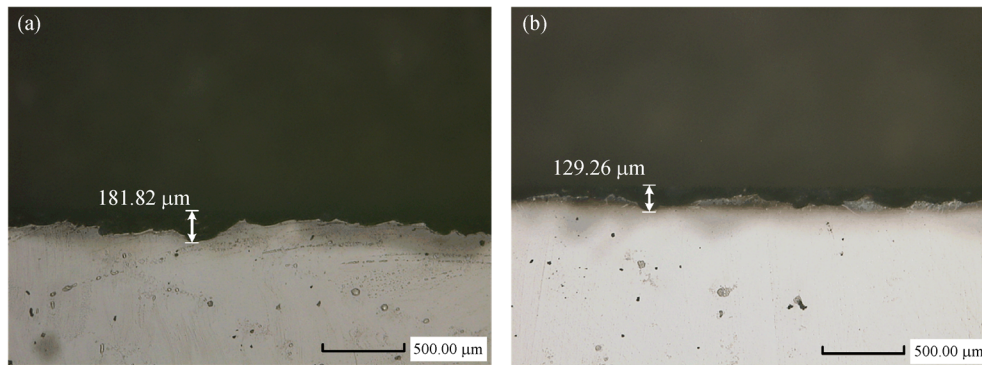


Fig. 10 Minimum chipping area in different laser scanning modes: (a) No. 12 in Table 4 (chipping area: $240524\ \mu\text{m}^2$); (b) No. 12 in Table 5 (chipping area: $216245\ \mu\text{m}^2$).

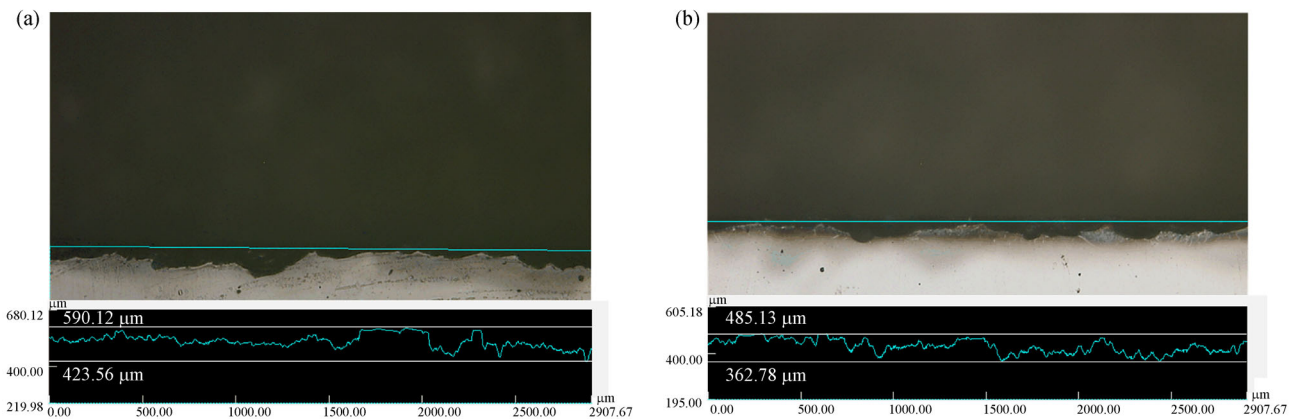


Fig. 11 Profile of the minimum chipping area in different laser scanning modes: (a) No. 12 in Table 4; (b) No. 12 in Table 5.

mode when it is optimal, and also, the overall fluctuation is small. This finding also means that the concentric circle scanning mode has a wider range of parameters for high-quality laser cutting solar float glass than its spiral counterpart.

4.5 Microstructure

The microstructure of the laser-processed sidewall has also been investigated through the images received from SEM as shown in Fig. 15. By comparing the best cutting

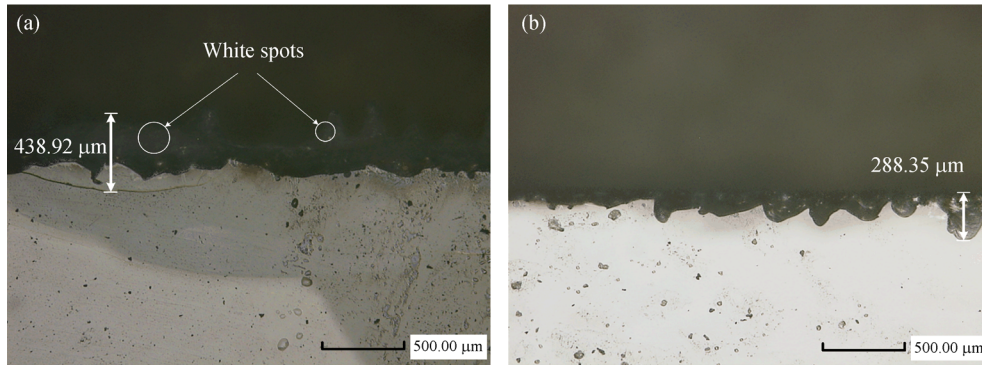


Fig. 12 Maximum chipping area in different laser scanning modes: (a) No. 15 in Table 4 (chipping area: $486664 \mu\text{m}^2$); (b) No. 6 in Table 5 (chipping area: $400168 \mu\text{m}^2$).

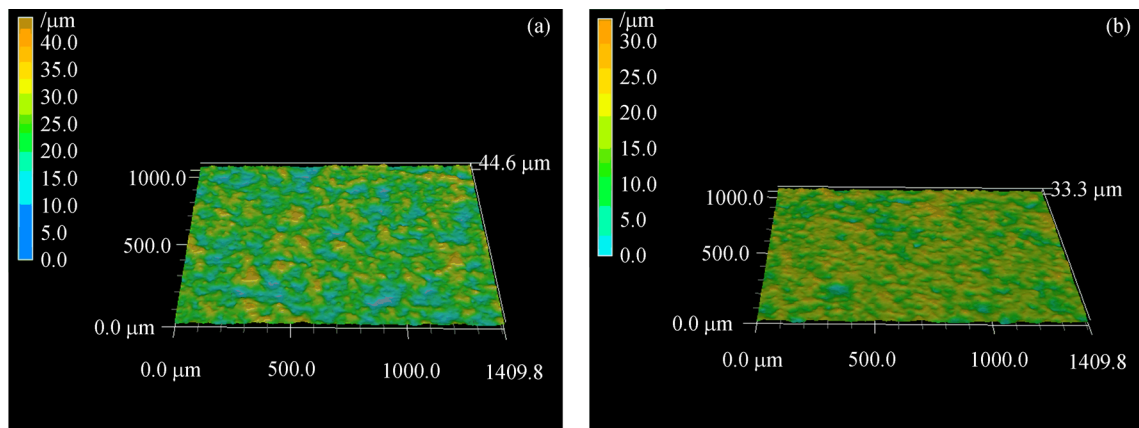


Fig. 13 Minimum Ra of the laser-processed sidewall in different laser scanning modes: (a) No. 14 in Table 4 (Ra : $3.59 \mu\text{m}$); (b) No. 8 in Table 5 (Ra : $2.92 \mu\text{m}$).

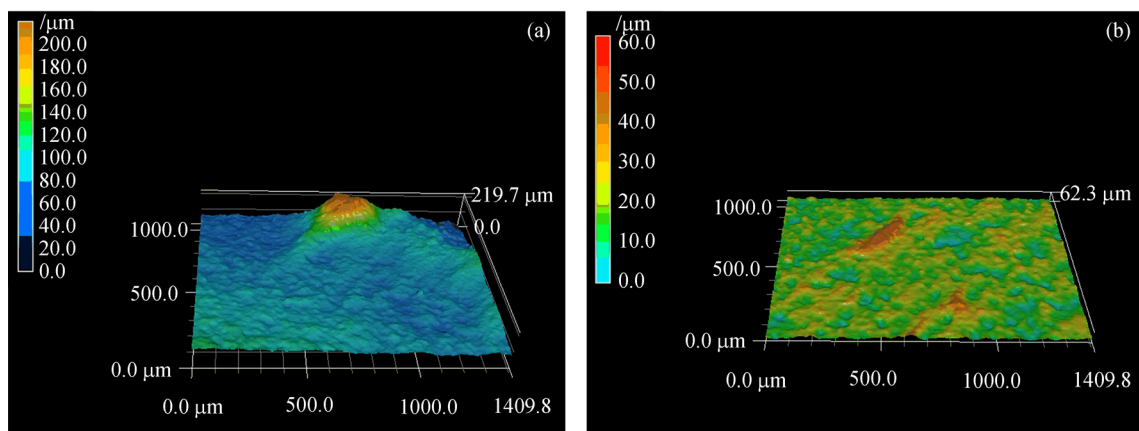


Fig. 14 Maximum Ra of the laser-processed sidewall in different laser scanning modes: (a) No. 16 in Table 4 (Ra : $11.16 \mu\text{m}$); (b) No. 15 in Table 5 (Ra : $4.91 \mu\text{m}$).

surfaces in the two scanning modes, the microscopic quality of the processed sidewall surface in the concentric circle scanning mode is better than that in the spiral scanning mode. Moreover, in the spiral scanning mode, the laser-processed surface had more microcracks, voids, and debris.

Figures 15(c) and 15(d) show the poor surface morphology of the two different scanning modes. In the concentric circle scanning mode, the laser-processed surface has several defects, such as voids and microcracks. However, in the spiral scanning mode, the surface is covered with a large area of fragmentation zone, and the glass damage in the area is very evident, which greatly reduces the quality of the glass cutting surface. Therefore, compared with the spiral scanning method, the cutting surface in the concentric circle scanning mode not only has a smaller surface roughness but also has fewer surface micro defects.

Figure 16 shows the chipping of the laser-processed surface edge in the two scanning modes. The edge chipping situation is the same as that in the vertical plane. For the spiral scanning mode, the uniformity of the chipping on the machined surface edge is poor, and the maximum chipping width is $97.63\ \mu\text{m}$, whereas in the concentric circle scanning mode, the chipping is more uniform and the maximum chipping is only $63.04\ \mu\text{m}$. In the case of poor cutting quality, Fig. 16(c) shows that the processed surface edge chipping width in the spiral scanning mode (maximum $195.36\ \mu\text{m}$) is still significantly greater than that in the concentric circle scanning mode

(maximum $144.12\ \mu\text{m}$). The processed surface near the chipping area is also covered with micro defects, such as microcracks and voids.

4.6 Element analysis

The main chemical element composition of the solar float glass substrate and the laser-processed sidewall surface (under different scanning modes) was examined through EDS. Figure 17 shows that the laser processing will not cause any pollution to the glass because this method is a non-contact processing one, so the element types have not changed before and after cutting. In terms of element content, regardless of the utilized laser scanning mode, the processed surface elements are close to the base material when the quality of the processed surface is good. However, in the spiral scanning method, the oxygen element on the laser-processed surface is reduced, and Na, Si, and Ca are increased, specifically Na. This event may reduce the mechanical strength, thermal stability, and chemical stability of the glass processed surface. Figure 17(d) shows the element content in the fragmentation area of the glass surface. Sodium and oxygen content increased significantly, and silicon and calcium content decreased, which greatly affected the surface processing quality.

5 Conclusions

This study mainly discusses two different laser scanning

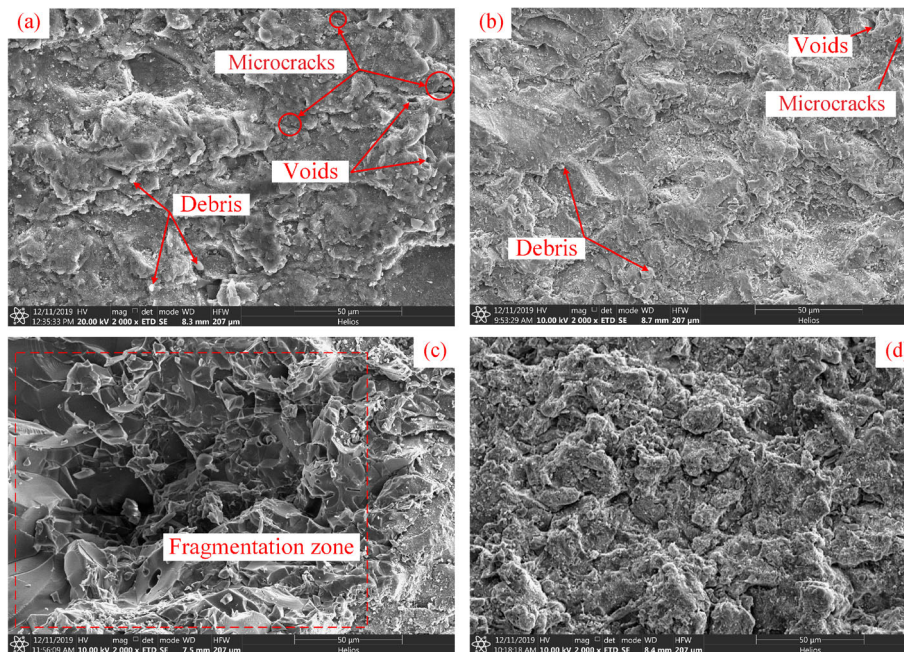


Fig. 15 SEM images of laser-processed sidewall surface in two different scanning modes: (a) No. 14 in Table 4; (b) No. 8 in Table 5; (c) No. 16 in Table 4; (d) No. 15 in Table 5.

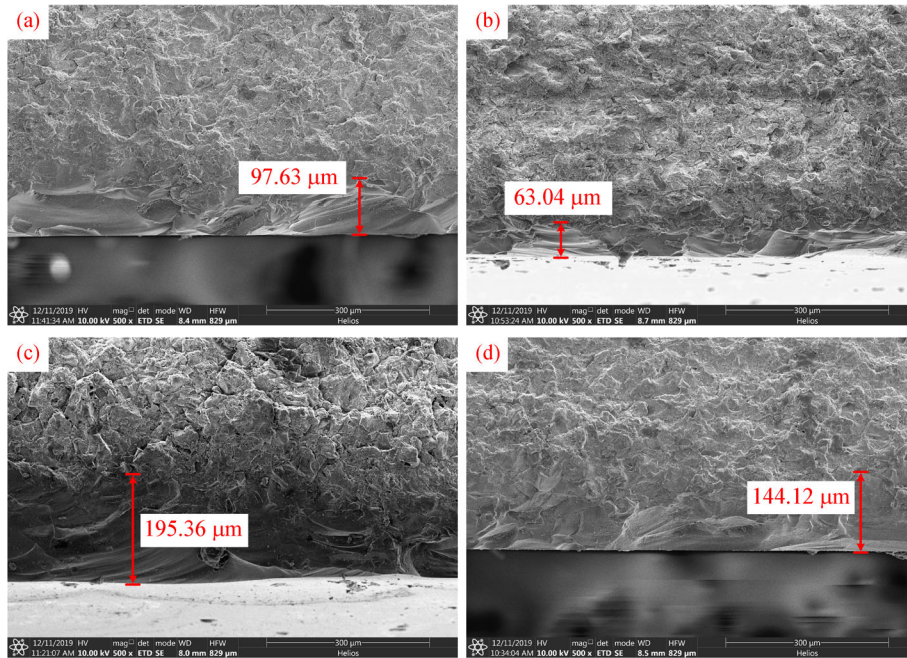


Fig. 16 SEM images of a laser-processed surface edge in two different scanning modes: (a) No. 12 in Table 4; (b) No. 12 in Table 5; (c) No. 15 in Table 4; (d) No. 6 in Table 5.

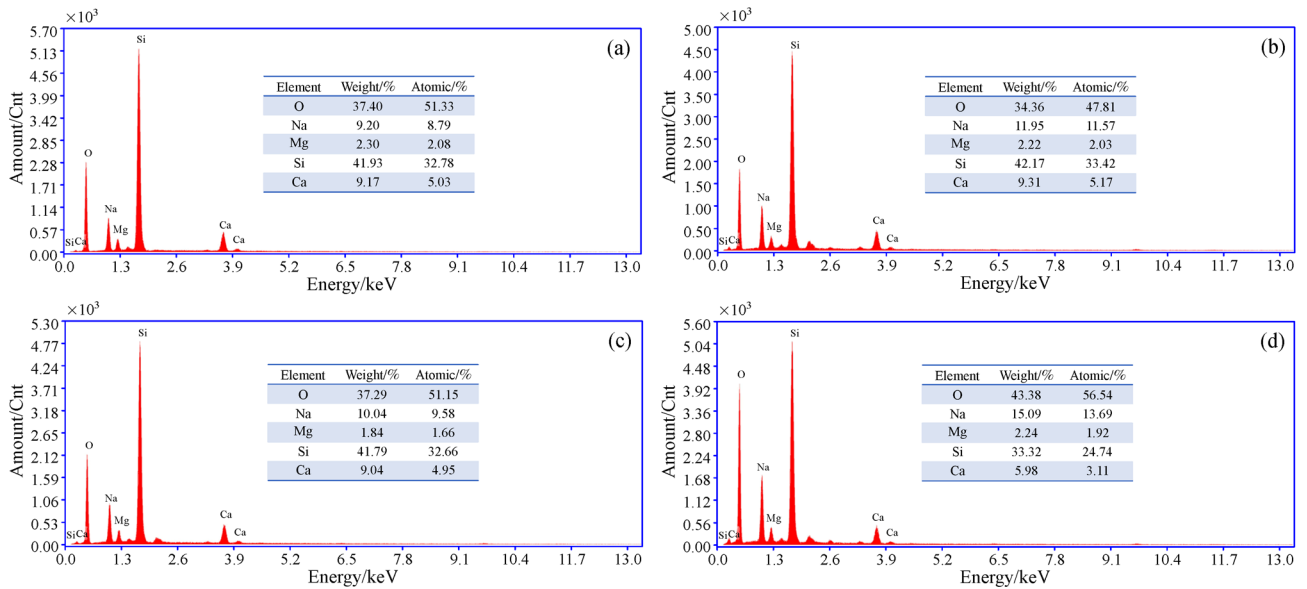


Fig. 17 EDS analysis of laser-processed surfaces on glass under two different scanning modes: (a) Glass substrate; (b) No. 14 in Table 4; (c) No. 8 in Table 5; (d) No. 16 in Table 4.

modes that can realize efficient laser cutting of solar float glass. The laser cutting quality and cutting efficiency under two scanning modes are compared and analyzed. From the above experiments and analysis, the following conclusions can be drawn:

1) The spiral and concentric circle scanning modes can achieve high-quality and high-efficiency solar glass cutting holes without additional treatment. However, the latter is better than the former in terms of cutting quality and efficiency. More specifically, the minimum area of edge

chipping, the smallest Ra of laser-processed surface, and minimal cutting time are reduced by 9.4%, 16.4%, and 14.2% in the concentric circle scanning mode, respectively.

2) The effect order of three parameters on the chipping area and Ra is $\gamma_w > \gamma_r > \gamma_v$ and $\gamma_r > \gamma_w > \gamma_v$, respectively, in the spiral scanning mode, and that in the concentric circle scanning mode is $\gamma_d > \gamma_v > \gamma_n$ for both indicators. The actual cutting efficiency in the spiral scanning mode depends on v (focus rise distance per layer remains constant), and the cutting efficiency in the concentric circle scanning mode is

not only related to v , but the n value substantially affects the cutting efficiency.

3) Compared with the spiral scanning mode, in the concentric circle scanning mode, not only the chipping area and cutting surface roughness are small, but also the degree of glass damage in the chipping area, and chipping is more uniform. The best combination of process parameters for two scanning modes is v (300 mm/s), w (0.6 mm), and r (65%); and v (2200 mm/s), n (6), and d (0.05), respectively. In this case, the concentric circle scanning mode can reduce the chipping area and sidewall surface roughness by 8.8% and 9.6% respectively at the same cutting efficiency.

4) In the concentric circle scanning mode, the three-dimensional cutting surface is smoother, and micro defects (micro cracks, voids, and debris) are fewer compared with the spiral scanning mode. If the laser cutting surface quality is great, then the element content of the laser-processed surface is close to the substrate under the concentric circle scanning mode.

Acknowledgements This work was supported by the National Natural Science Foundation of China (Grant No. 51905191), the Major Project of Science and Technology Innovation Special Project for Hubei Province (Grant No. 2018AAA027), and Wuhan Science and Technology Planning Project (Grant No. 201903070311520).

References

1. Yang L J, Wang Y, Tian Z G, et al. YAG laser cutting soda-lime glass with controlled fracture and volumetric heat absorption. *International Journal of Machine Tools and Manufacture*, 2010, 50 (10): 849–859
2. Kühnapfel S, Severin S, Kersten N, et al. Multi crystalline silicon thin films grown directly on low cost soda-lime glass substrates. *Solar Energy Materials and Solar Cells*, 2019, 203: 110168
3. Kondrashov V I, Shitova L A, Litvinov V A, et al. Characteristics of cutting parameters and their effect on the glass edge quality. *Glass and Ceramics*, 2001, 58(9–10): 303–305
4. Matsumura T, Hiramatsu T, Shirakashi T, et al. A study on cutting force in the milling process of glass. *Journal of Manufacturing Processes*, 2005, 7(2): 102–108
5. Zhimalov A B, Solinov V F, Kondratenko V S, et al. Laser cutting of float glass during production. *Glass and Ceramics*, 2006, 63(9–10): 319–321
6. Sharma A, Jain V, Gupta D. Characterization of chipping and tool wear during drilling of float glass using rotary ultrasonic machining. *Measurement*, 2018, 128: 254–263
7. Azmir M A, Ahsan A K. A study of abrasive water jet machining process on glass/epoxy composite laminate. *Journal of Materials Processing Technology*, 2009, 209(20): 6168–6173
8. Yu X, Wang P, Li X, et al. Thin Czochralski silicon solar cells based on diamond wire sawing technology. *Solar Energy Materials and Solar Cells*, 2012, 98: 337–342
9. Lumley R M. Controlled separation of brittle materials using a laser. *American Ceramic Society Bulletin*, 1969, 48(9): 850–854
10. Nisar S, Li L, Sheikh M A. Laser glass cutting techniques—A review. *Journal of Laser Applications*, 2013, 25(4): 042010
11. Tsai C H, Liou C S. Fracture mechanism of laser cutting with controlled fracture. *Journal of Manufacturing Science and Engineering*, 2003, 125(3): 519–528
12. Udrea M V, Alacakar A, Esendemir A, et al. Small-power-pulsed and continuous longitudinal CO₂ laser for material processing. *Proceedings Volume 4068, SIOEL'99: Sixth Symposium on Optoelectronics*, 2000, 4068: 657–662
13. Zhao C, Zhang H, Wang Y. Semiconductor laser asymmetry cutting glass with laser induced thermal-crack propagation. *Optics and Lasers in Engineering*, 2014, 63: 43–52
14. Deng L, Yang H, Zeng X, et al. Study on mechanics and key technologies of laser nondestructive mirror-separation for KDP crystal. *International Journal of Machine Tools and Manufacture*, 2015, 94: 26–36
15. Kuo Y L, Lin J. Laser cleaving on glass sheets with multiple laser beams. *Optics and Lasers in Engineering*, 2008, 46(5): 388–395
16. Jiao J, Wang X. Cutting glass substrates with dual-laser beams. *Optics and Lasers in Engineering*, 2009, 47(7–8): 860–864
17. Zhao C, Zhang H, Yang L, et al. Dual laser beam revising the separation path technology of laser induced thermal-crack propagation for asymmetric linear cutting glass. *International Journal of Machine Tools and Manufacture*, 2016, 106: 43–55
18. Wang H, Wang M, Zhang H, et al. Use of inner-heated circular microwave spot to cut glass sheets based on thermal-controlled fracture method. *Journal of Materials Processing Technology*, 2020, 276: 116309
19. Gattass R R, Mazur E. Femtosecond laser micromachining in transparent materials. *Nature Photonics*, 2008, 2(4): 219–225
20. Shin H, Kim D. Cutting thin glass by femtosecond laser ablation. *Optics & Laser Technology*, 2018, 102: 1–11
21. Couairon A, Mysyrowicz A. Femtosecond filamentation in transparent media. *Physics Reports*, 2007, 441(2–4): 47–189
22. Chuang C F, Chen K S, Chiu T C, et al. Crafting interior holes on chemically strengthened thin glass based on ultrafast laser ablation and thermo-shock crack propagations. *Sensors and Actuators A: Physical*, 2020, 301: 111723
23. Mačernytė L, Skruibis J, Vaičaitis V, et al. Femtosecond laser micromachining of soda-lime glass in ambient air and under various aqueous solutions. *Micromachines*, 2019, 10(6): 354
24. Collins A R, O'Connor G M. Mechanically inspired laser scribing of thin flexible glass. *Optics Letters*, 2015, 40(20): 4811–4814
25. Liu P, Duan J, Wu B, et al. A flexible multi-focus laser separation technology for thick glass. *International Journal of Machine Tools and Manufacture*, 2018, 135: 12–23
26. Liu P, Deng L, Zhang F, et al. Study on high-efficiency separation of laminated glass by skillfully combining laser-induced thermal-crack propagation and laser thermal melting. *Applied Physics A*, 2020, 126(4): 286
27. Feucht F, Ketelaer J, Wolff A, et al. Latest machining technologies of hard-to-cut materials by ultrasonic machine tool. *Procedia CIRP*, 2014, 14(1): 148–152